Meas. Sci. Technol. **20** (2009) 115104 (6pp) doi:10.1088/0957-0233/20/11/115104

Step-edge calibration of torsional sensitivity for lateral force microscopy

Onejae Sul and Eui-Hyeok Yang

Department of Mechanical Engineering, Stevens Institute of Technology, Castle Point on Hudson, Hoboken, NJ 07030, USA

E-mail: Eui-Hyeok.Yang@steves.edu

Received 10 August 2009, in final form 26 August 2009
Published 25 September 2009
Online at stacks.iop.org/MST/20/115104

Abstract
A novel calibration technique has been developed for lateral force microscopy (LFM). Typically, special preparation of the atomic force microscope (AFM) cantilever or a substrate is required for LFM calibration. The new calibration technique reported in this paper greatly reduces the required preparation processes by simply scanning over a rigid step and measuring the response of the AFM photodiode in the normal and lateral directions. When an AFM tip touches a step while scanning, the tip experiences a reaction force from the step edge, and the amount of torsion can be estimated based on the ratio of the normal and torsional spring constants of an AFM cantilever. Therefore, the torsion can be calibrated using the measured response of the photodiode from the lateral movement of the AFM tip. This new calibration technique has been tested and confirmed by measuring Young's modulus of a nickel (Ni) nanowire.

Keywords: lateral force microscopy, nanowire, atomic force microscopy

(Some figures in this article are in colour only in the electronic version)

1. Background

Lateral force microscopy (LFM) is widely used for frictional measurements on substrates, using the response of the photodiode generated by the torsion of AFM cantilevers. Because of the scientific importance, many variant LFM techniques [1–15] were developed to calibrate the lateral force, representatively in the Cleveland and Sader methods [1, 2], and also there was quantitative comparison among the techniques [3, 4]. If the AFM cantilever undergoes torsion, the laser reflected off the back of the cantilever will change position on the photodiode. The photodiode is divided into four areas. The movement of the laser spot across the left and right halves of the photodiode (L–R) can detect this cantilever torsion. Likewise, the top and bottom halves of the diode (T–B) can detect cantilever deflection in the normal direction. Therefore, one can obtain the amount of AFM cantilever torsion by the measurement of L–R voltage if the response of the L–R is pre-calibrated. Unlike the sensitivity calibration in the normal direction, the torsional calibration is not straightforward, and therefore requires the incorporation of special techniques including the use of a hard colloidal sphere glued at the tip of the cantilever [3, 6–10], knowledge of the geometry between the cantilever and photodiode [11], a wedge-shaped substrate [12], a lever attached to an AFM cantilever [13] or an upward sharp tip [14]. While several methods reported previously relied on the ratios of the normal and torsional spring constants of an AFM cantilever [12–14], the aforementioned techniques, except for torsional vibration methods [5, 6], require a specially prepared AFM cantilever or a substrate. The new lateral calibration technique described in this paper has relatively simpler preparation steps than existing methods since it does not require colloidal sphere or lever gluing, knowledge of geometries between the AFM cantilever and the photodiode or special crystal preparation.

2. Step-edge calibration for lateral force microscopy

This section describes the calibration of the lateral force. In the initial pre-calibration step (section 2.1), the photodiode responses in the normal and lateral directions were calibrated with a known deflection and torsion. As will be described in

section 2.2, the lateral force can then be determined from the known amount of torsion when the AFM tip touches the step edge. Finally, a conversion factor from the lateral photodiode response to the lateral force was obtained.

2.1. Pre-calibration of the photodiode responses with deflection and torsion

To accurately determine the lateral force, the response of the photodiode in each direction should be pre-calibrated first, especially considering nonlinearity [15]. Here, the conversion equation can be obtained on the normal (or lateral) photodiode signal variation ΔI_{T-B} (or I_{L-R}) with the deflection z (or torsion δ). Normal deflection pre-calibration is straightforward and thus is more accurate than that for torsion. When the AFM tip is depressed against a rigid flat surface, the deflection of the tip, z, is identical to the variation of the piezoelectric actuator's depression movement. A calibration value for I_{T-B} versus the normal deflection can be obtained from the force–distance curves. In this measurement, the value is

$$\Delta I_{T-B}\ (\mathrm{mV}) = 6.4 \pm 0.1\ (\mathrm{mV\ nm^{-1}}) \times z\ (\mathrm{nm}) \tag{1}$$

with the normal response found to be close to linear, only deviating from this in the upper scan range by 2% in the scan limit (figure 1(*a*)).

Torsional pre-calibration, ΔI_{L-R} against torsion δ, is performed by scanning the AFM tip laterally on a silicon dioxide substrate. When the cantilever is depressed against a rigid substrate, it experiences torsion in addition to the normal deflection from the reactive force from the substrate. The amount of torsion (also the inclination angle, ψ, and the *L–R* voltage, I_{L-R}) depends on the depression of the cantilever. If the tip is moving in one direction or the other, the response of the photodiode, I_{L-R}, swings between two values around an offset (figures 1(*b*) and (*c*)). The difference between the two values depends on the amount of depression.

While the AFM tip is laterally scanning, it has an inclination angle, ψ. There are three forces acting at the AFM tip: the reaction force from vertical deflection, f_{Normal}, friction, f_μ, and the reaction force from torque, f_{Torsion}. The three forces balance so that the AFM cantilever becomes stable against torsion:

$$f_{\mathrm{Normal}} \sin\psi + f_\mu \cos\psi = f_{\mathrm{Torsion}}. \tag{2}$$

Each component of force is [16]

$$f_{\mathrm{Normal}} = \frac{Et^3 w}{4L^3} z \tag{3}$$

$$f_\mu = \mu \cdot f_{\mathrm{Normal}}, \tag{4}$$

$$f_{\mathrm{Torsion}} = \frac{Et^3 w}{3(1+\nu)Lh} \psi \tag{5}$$

where t, w, L, h are respectively thickness (2.0 ± 0.5 μm), width (50 ± 5 μm), length (450 ± 10 μm) and tip height (10 ± 1 μm) of the AFM cantilever (Nanoworld, ContPt), and E (160 GPa [17]) and ν (0.27 [17]) are Young's modulus and Poisson's ratio of silicon respectively. The frictional coefficient of silicon dioxide is 0.05 [18]. Then equation (2) gives

$$\frac{\psi}{\sin\psi + \mu\cos\psi} = \frac{3h(1+\nu)}{4L^2} z. \tag{6}$$

The amount of torsion δ is calculated using the equation

$$\delta = \psi \cdot h, \tag{7}$$

where the amount of z-piezo depression is assumed to be identical to the normal deflection, z. Thus from equations (6) and (7), a depression z can be converted into torsion δ.

To experimentally determine the relationship between the torsion and I_{L-R}, lateral scans were performed for various depression depths controlled by the z-piezo in 640 nm steps, starting from approximately 0 nm (barely touching the substrate) up to 5440 nm. From equations (6) and (7), the maximum torsion was determined to be 0.8 ± 0.1 nm at 5440 nm depression. As expected, the half range of I_{L-R} increased following an increase of the depression depth (figure 1(*d*)). The response of the photodiode was linear at small depressions, but it became strongly nonlinear at deep depressions. The origin of this nonlinearity can be partly from the nonlinear response of the photodiode and partly from the limit of the AFM cantilever's ability to twist at large depressions, where then it responds only with increased deflection at its tip. The measurement was fitted to a trial exponential function, which was found to follow the experimental data accurately:

$$\Delta I_{L-R}\ (\mathrm{mV}) = 1017 \pm 25\ \mathrm{mV} - 629 \pm 26\ \mathrm{mV} \times \exp(-\delta(\mathrm{nm})/0.29 \pm 0.04\ \mathrm{nm}). \tag{8}$$

Consequently, δ can be found when a value for ΔI_{L-R} is given.

2.2. Step calibration of the lateral force

In this section, a conversion factor α relating ΔI_{L-R} to the lateral force is determined. If a force is applied at the AFM tip, then the responses ΔI_{T-B} and ΔI_{L-R} would be recorded. ΔI_{T-B} would be converted into z and δ. Finally, the lateral force can be calculated from the torsional spring constant for calibration by ΔI_{L-R}.

If an arbitrary amount of force against a step in the substrate is applied to an AFM tip, the force can be divided into two components, normal and torsional (figure 2), generating tip movements in both directions. In this situation, the friction force from the step edge provides an additional force against the AFM tip. We prepared silicon dioxide steps by etching a wafer using deep reactive ion etching. The step height was about 5 μm so that during the scan the AFM tip would not touch the bottom of the substrate. The height of the tip was raised so that only the very tip (within 640 nm) was touching the step. From figure 2, the reaction forces (f_{Torsion} and f_{Normal}) and the friction force (f_μ) can be divided into x and z directions:

$$f_{\mathrm{Torsion}} = f_{\mathrm{Total}} \cos\theta, \qquad f_{\mathrm{Normal}} = f_{\mathrm{Total}} \sin\theta$$
$$\text{and} \qquad f_\mu = f_{\mathrm{Total}} \cdot \mu, \tag{9}$$

where θ is the slope angle of the AFM tip. The angle was measured by using an SEM image taken on the AFM tip and

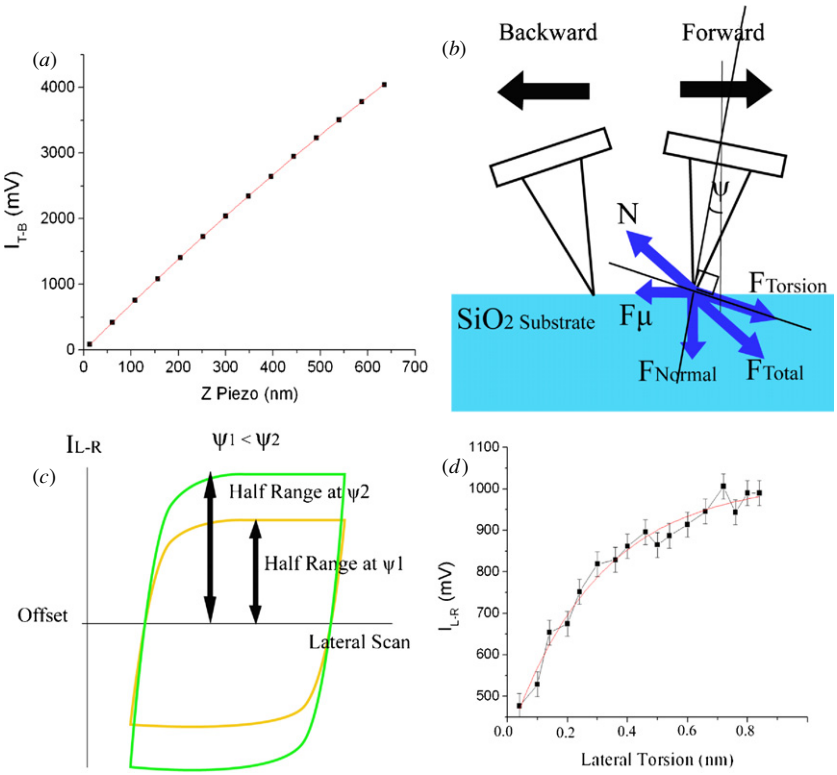

Figure 1. (*a*) Normal direction photodiode response depending on the depression depth. The measurement error was 20 mV. (*b*) The reaction force in the normal direction added with the friction force, f_μ, will balance the lateral force, f_{Torsion}, which results in stable inclination angle, ψ. (*c*) If the tip is depressed harder, the variation width (half range) of the lateral response swing will increase along with the torsion. (*d*) Measured half range depending on lateral torsion. The curve is a fit to the measurements. The measurement error was 50 mV.

it was $20 \pm 1^\circ$. The AFM cantilever reacts as a spring in both directions against the two components of forces:

$$f_{\text{Torsion}} + f_\mu \sin\theta = k_{\text{Torsion}} \cdot \delta \qquad \text{and}$$
$$f_{\text{Normal}} - f_\mu \cos\theta = k_{\text{Normal}} \cdot z. \tag{10}$$

We then have a relationship between δ and z as follows:

$$\delta = \frac{k_{\text{Normal}}}{k_{\text{Torsion}}} \frac{\cos\theta + \mu \sin\theta}{\sin\theta - \mu \cos\theta} z. \tag{11}$$

The normal deflection by an arbitrary force is determined accurately by measuring I_{T-B} and calculated in equation (1), where I_{T-B} is the *T–B* voltage (usually called the 'error' channel in the AFM data acquisition). Figure 2(*b*) shows the variation of the *T–B* voltage, *z*-piezo and *L–R*, when the AFM tip touches a step edge. The AFM tip was not in contact with the bottom surface, the scan rate was 1 μm s^{-1} and the feedback was on. During a lateral scan of 180 nm from the time of contact, the *T–B* voltage varies by 3429 $\pm$ 20 mV. This means that the AFM tip is deflected by 537 $\pm$ 3 nm. The feedback mechanism of the AFM system does not yet (figure 2(*b*), middle panel) respond during the scanning because of the delays in the feedback circuits, so the *z*-piezo does not move at all. Therefore, the net deflection z of the AFM tip is also 537 $\pm$ 3 nm.

From equations (3) and (5), the ratio of the two spring constants is

$$\frac{k_{\text{Normal}}}{k_{\text{Torsional}}} = \frac{3(1+\nu)}{4} \left(\frac{h}{L}\right)^2. \tag{12}$$

Then from equations (11) and (12), the estimated tip torsion is

$$\delta = \frac{k_{\text{Normal}}}{k_{\text{Torsion}}} \frac{z}{\tan\theta} = \frac{3(1+\nu)}{4} \left(\frac{h}{L}\right)^2 \frac{\cos\theta + \mu \sin\theta}{\sin\theta - \mu \cos\theta} z. \tag{13}$$

When the deflection $z = 537$ nm is put into equation (13), the torsion δ is determined to be 0.5 ± 0.1 nm. This is recorded as a voltage of $I_{L-R} = 918 \pm 20$ mV in the *L–R* channel, and this agrees well with the lateral pre-calibration result, equation (8) in section 2.1. The torsional spring constant can be obtained once the normal spring constant is measured. The normal spring constant can be calculated from equation (3), but direct measurement would give a more accurate value. By measuring the resonance frequency of the AFM cantilever, $\omega_0 = 8.0 \pm 0.1$ kHz, where $\omega_0 = \sqrt{k_{\text{Normal}}/m}$ and m is the mass of the AFM cantilever, k_{Normal} was calculated as 0.19 ± 0.05 nN nm^{-1}, which produces k_{Torsion} as 403 ± 163 nN nm^{-1}. Then the lateral force is

$$f_{\text{Torsion}} = k_{\text{Torsion}} \cdot \delta = 201 \pm 81 \text{ nN}. \tag{14}$$

Finally, the conversion factor α from I_{L-R} to f_{Torque} can be determined:

$$\alpha = \frac{f_{\text{Torsion}}}{I_{L-R}} = 0.21 \pm 0.09 \text{ nN mV}^{-1}. \tag{15}$$

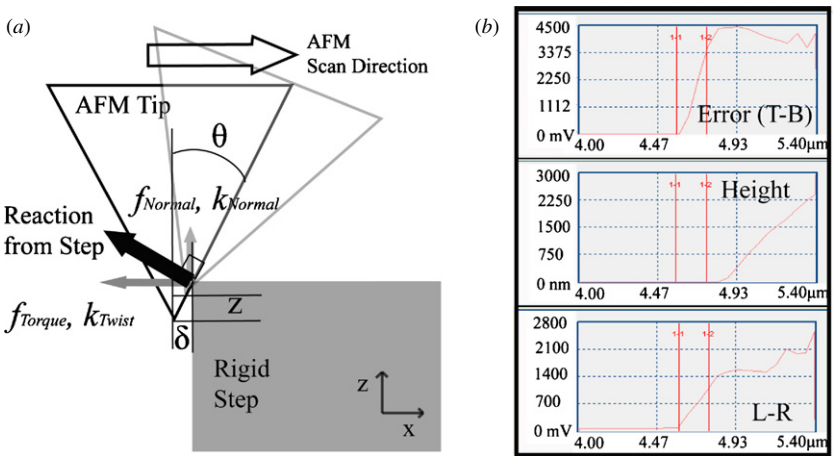

Figure 2. Reaction force of a rigid step edge and the response of the photodiode. (*a*) Reaction force from a step can be divided into two components, f_{Normal} and f_{Torque}. (*b*) *T–B* voltage, *z*-piezo depth and *L–R* voltage while the AFM tip scans over a step. In each channel, only the measurements between the two red (central) lines were used for torsion estimation. The location of the left red line is the moment of touch.

3. Measurement of Young's modulus of Ni nanowires

To verify the validity of the calibration method, lateral force microscopy has been used to measure Young's modulus of a nickel (Ni) nanowire. One assumption here is that torsion δ is much smaller than the lateral scanning distance, Δ, so that Δ can be treated the same as the deflection of the polymer wire. This can be justified easily because the magnitude of the AFM tip torsion is on the order of nanometers while the observed Ni nanowire deflection would be on the order of microns. With a beam deflection amount Δ and a known force f applied at its tip, Young's modulus of the nanowire is calculated from elastic beam bending theory [19]:

$$E = \frac{4fL^3}{3\pi r^4 \Delta}, \tag{16}$$

where L and r are the length and radius of the nanowire respectively. The AFM tip is scanned laterally from an arbitrary location away from the nanowire (figure 3). At this time, because the LFM is calibrated, there is no need to use the *T–B* channel, so the feedback was turned off. Figure 3(*c*) shows the expected *L–R* voltage across a nanowire. A gradual increase of the *L–R* voltage is observed if there is contact between the AFM and the nanowire. After some time, the AFM tip is released, and *L–R* returns to the original bias.

Ni nanowires were grown inside commercially available anodized alumina oxide (AAO) (Whatman Ltd) membranes by electrochemical deposition [20]. First, thin metal films such as Au and Ag were coated on one side of the AAO membrane and used as the metal electrode for electroplating. Ni electrolyte was composed of 30 g of $NiSO_4 \cdot 6H_2O$, 4.5 g of $NiCl_2 \cdot 6H_2O$ and 4.5 g of H_3BO_3 in 100 ml of deionized water. The membranes with a nominal pore size of 200 nm were used to grow 250–300 nm diameter nanowires. Applied currents were 1–2 mA cm^{-2} through the platinized titanium anode (Stan Rubinstein Assoc. Inc.) and kept constant using a galvanostat (263 A-1, Princeton Applied Research, AMETEK Inc) during the entire electrochemical deposition period. The growth rate and the length of Ni nanowires were controlled

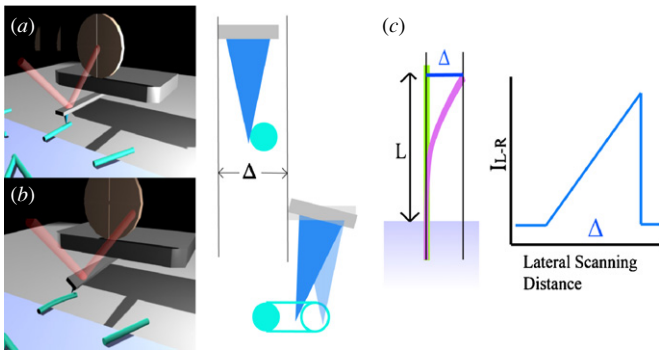

Figure 3. Distortion of a Ni nanowire during lateral force microscopy. The AFM cantilever distortion is exaggerated for clarity. (*a*) Before the AFM tip touches the Ni nanowire, there is no distortion of the AFM cantilever and the laser reflection is at the center of the photodiode. (*b*) When the AFM head moves laterally by Δ_0, the AFM cantilever distorts by an amount δ and the reflection is now biased in one lateral direction (front view schematics on the right). (*c*) Schematic comparison of *L–R* voltage generated from the photodiode, when the AFM tip deflects the Ni wire at its tip.

by both the applied current and the deposition time, which was confirmed by an optical microscope (Hi-scope advanced KH3000, Hirox) and a scanning electron microscope (SEM, Phillips, XL-40). After deposition and the dissolution of the AAO membrane in 5 M sodium hydroxide (NaOH), Ni nanowires were collected as a suspension and cleaned several times. One drop of the suspension was placed on a silicon substrate. After evaporation of the solution, the substrate was broken to find cantilevered Ni nanowires with an optical microscope. To hold the individual nanowires, nominally 300 nm thickness of Ni film was deposited using an electron beam evaporator. Thus, only the cantilevered portion of a nanowire would respond to the lateral force microscopy. Upon finding individual Ni cantilever nanowires, they were brought under the AFM system (Pacific Nanotechnology). The circular cross-sections of individual Ni nanowires were verified using scanning electron microscope images.

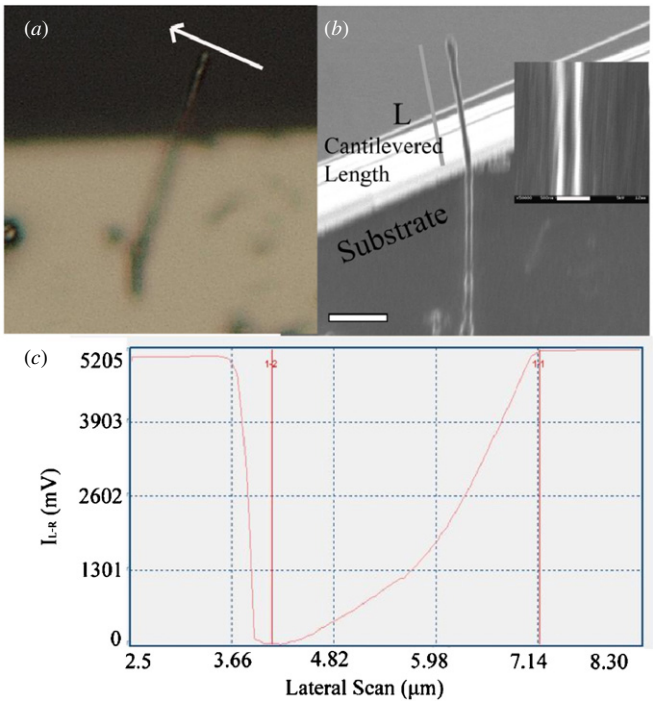

Figure 4. (*a*) Optical microscope image of a Ni nanowire. The arrow displays the LFM scan direction. (*b*) A scanning electron microscope image of the same nanowire. The nanowire has been bent due to repeated measurement. The scale bar is 5 μm. (Inset: a circular cross-section of a Ni nanowire showing its diameter, 360 $\pm$ 70 nm, after Ni film deposition. Scale bar is 500 nm.) (*c*) LFM scan in the *L–R* channel while applying a force at the tip of the nanowire in (*a*). Note that because of the scan direction, the polarity of the signal variation is a mirror image of that shown in figure 3(*c*).

From the I_{L-R} and Δ measurements (figure 4), $\Delta I_{L-R} = 5155 \pm 20$ mV is obtained with $\Delta = 3.0 \pm 0.4$ μm at the nanowire tip. Given the length and diameter of the nanowires as 11 $\pm$ 1 μm and 360 $\pm$ 70 nm, respectively, Young's modulus is found from equation (16) to be 185 $\pm$ 68 GPa. The measurement is smaller than the bulk Young's modulus of Ni (200 GPa), but there are several reports on Young's modulus of the electroplated thin Ni films that range from 85 GPa to 205 GPa [21–24] depending on the current density and the electroplating temperature. Our growth conditions, low current density (1–2 mA cm^{-2}) and room temperature environment, generate Young's modulus of nickel wires close to the bulk value (150–205 GPa) [21]; therefore, our measurement on Ni nanowire agrees with their results and confirms the validity of the self-edge calibration technique.

4. Conclusion

A step-edge calibration technique has been developed for use with lateral force microscopy. This method eliminates the need of any special preparation on the AFM cantilever tip for lateral force microscopy. Scanning the AFM tip over a rigid step supplies sufficient information to estimate the amount of AFM tip torsional deflection. The AFM tip response under a lateral force has been calculated using this principle. This new step scanning technique can be used for any kind of AFM cantilever as long as one knows the two individual spring constants (torsion and normal). The measurement process reported here has been confirmed by measuring Young's modulus of a Ni nanowire.

Acknowledgments

This work has been partially supported by the National Science Foundation Major Research Instrumentation Program, award no DMI-0619762, and the Air Force Office for Scientific Research (award no FA9550-08-1-0134).

References

[1] Cleveland J P, Manne M, Bocek D and Hansma P K 1993 A nondestructive method for determining the spring constant of cantilevers for scanning force microscopy *Rev. Sci. Instrum.* **64** 403
[2] Sader J E, Chon J W M and Mulvaney P 1999 Calibration of rectangular atomic force microscope cantilevers *Rev. Sci. Instrum.* **70** 3967
[3] Cain R G, Reitsma M G, Biggs S and Page N W 2001 Quantitative comparison of three calibration techniques for the lateral force microscope *Rev. Sci. Instrum.* **72** 3304
[4] Pettersson T, Nordgren N, Rutland M W and Feiler A 2007 Comparison of different methods to calibrate torsional spring constant and photodetector for atomic force microscopy friction measurements in air and liquid *Rev. Sci. Instrum.* **78** 093702
[5] Jeon S, Braiman Y and Thundat T 2004 Torsional spring constant obtained for an atomic force microscope cantilever *Appl. Phys. Lett.* **84** 1795
[6] Tocha E, Song J, Schoherr H and Vancso G J 2007 Calibration of friction force signals in atomic force microscopy in liquid media *Langmuir* **23** 7078
[7] Cannara R J, Eglin M and Carpick R W 2006 Lateral force calibration in atomic force microscopy: a new lateral force calibration method and general guidelines for optimization *Rev. Sci. Instrum.* **77** 053701
[8] Green C P, Lioe H, Cleveland J P, Proksch R, Mulvaney P and Sader J E 2004 Normal and torsional spring constants of atomic force microscope cantilevers *Rev. Sci. Instrum.* **75** 1988
[9] Ecke S, Raiteri R, Bonaccurso E, Reiner C, Deiseroth H-J and Butt H-J 2001 Measuring normal and friction forces acting on individual fine particles *Rev. Sci. Instrum.* **72** 4164
[10] Cain R G, Biggs S and Page N W 2000 Force calibration in lateral force microscopy *J. Colloid Interface Sci.* **227** 55
[11] Liu E, Blanpain B and Celis J P 1996 Calibration procedures for frictional measurements with a lateral force microscope *Wear* **192** 141
[12] Ogletree D F, Carpick R W and Salmeron M 1996 Calibration of frictional forces in atomic force microscopy *Rev. Sci. Instrum.* **67** 3298
[13] Feiler A, Attard P and Larson I 2000 Calibration of the torsional spring constant and the lateral photodiode response of frictional force microscopes *Rev. Sci. Instrum.* **71** 2746
[14] Bogdanovic G, Meurk A and Rutland M W 2000 Tip friction—torsional spring constant determination *Colloids Surf.* B **19** 397

[15] Schaffer T E 2002 Force spectroscopy with a large dynamic range using small cantilevers and an array detector *J. Appl. Phys.* **91** 4739
[16] Gibson C T, Watson G S and Myhra S 1997 Lateral force microscopy a quantitative approach *Wear* **213** 72
[17] Hess P 1996 Laser diagnostics of mechanical and elastic properties of silicon and carbon films *Appl. Surf. Sci.* **106** 433
[18] Stevens K M 1996 *IEEE Micro Electro Mechanical Systems Workshop (San Diego, CA)* p 97
[19] Fenner R T 1989 *Mechanics of Solids* (Boca Raton, FL: CRC Press)
[20] Routkevitch D, Tager A A, Haruyama J, Almawlawi D, Moskovits M and Xu J M 1996 Nonlithographic nano-wire arrays: fabrication, physics, and device applications *IEEE Trans. Electron Devices* **43** 1646
[21] Luo J K, Flewitt A J, Spearing S M, Fleck N A and Milne W I 2004 Young's modulus of electroplated Ni thin film for MEMS applications *Mater. Lett.* **58** 2306
[22] Kim S H and Boyd J G 2006 A new technique for measuring Young's modulus of electroplated nickel using AFM *Meas. Sci. Technol.* **17** 2343
[23] Fritz T, Griepentrog M, Mokwa W and Schnakenberg U 2003 Determination of Young's modulus of electroplated nickel *Electrochim. Acta* **48** 571
[24] Zhou Z M, Zhou Y, Yang C S, Chen J A, Ding G F, Ding W, Wang M J and Jang Y M 2004 The evaluation of Young's modulus and residual stress of nickel films by microbridge testings *Meas. Sci. Technol.* **15** 2389